J. Am. Chem. Soc. 1984, 106, 639-644

Electronic Structures of the $(\eta^5\text{-}C_5H_5)_2TiL_2$ Complexes (L = F, Cl, Br, I, CH_3)

Mitchell R. M. Bruce, Almus Kenter, and David R. Tyler*

Contribution from the Department of Chemistry, Columbia University, New York, New York 10027.
Received April 22, 1983

Abstract: The self-consistent-field–Xα–scattered-wave (SCF–Xα–SW) molecular orbital method was used to investigate the electronic structures of the Cp_2TiL_2 (Cp = η^5-C_5H_5; L = F, Cl, Br, I, CH_3) complexes. Emphasis was placed on identifying the lowest energy electronic excited states of these complexes. For L = F, Cl, and Br the lowest energy electronic transitions are predicted to be Cp → Ti charge-transfer transitions. The halide → Ti charge-transfer transitions occur at higher energy. For L = I, Cp → Ti and I → Ti charge-transfer transitions are predicted to be very close in energy; the photoelectron spectroscopy work of others suggests that the I → Ti transitions will be the lowest energy transitions. When L = CH_3, the two lowest energy excited states involve excitation of electrons from Ti–CH_3 bonding orbitals to a Ti d orbital. That the fluoride, chloride, and bromide complexes have lowest energy excited states different from those of the iodide and methyl complexes is reflected in the photochemistry of the two types of complexes. In the former complexes, Cp–Ti bond cleavage results upon low-energy irradiation; in the latter complexes, Ti–L bond cleavage occurs when the complexes are irradiated.

We have been studying the photochemical reactivity of ligand-to-metal charge-transfer (LMCT) excited states of organometallic complexes. Our interest in these excited states stems from a belief that LMCT excitation will be useful in reducing organometallic complexes;[1] the other types of charge-transfer excited states of organometallic complexes (metal-to-ligand charge transfer (MLCT) and charge transfer to solvent) typically lead to metal complex oxidation.[2] A problem arises in the study of LMCT photochemistry because the vast majority of organometallic complexes have metals in low oxidation states. As a consequence, LMCT transitions usually occur at very high energies in organometallic complexes and they are difficult to identify because they overlap with numerous MLCT and other bands.[3] Such conditions make it difficult to study the photochemistry of LMCT excited states because of the interference from other excited-state reactivities. Ideally, for a photochemical study, the LMCT absorption bands should be the lowest energy bands in the electronic spectrum and they should be well separated from other bands. Thus, our strategy for studying the photochemistry of LMCT excited states is to study very high oxidation state organometallic complexes. For simple Coulombic reasons the LMCT transitions in such complexes will occur at a much lower energy than do the LMCT transitions of typical low oxidation state complexes.[4] For similar reasons, the MLCT transitions in the high oxidation complexes will occur at a higher energy than they do in the low oxidation state complexes.

Once we had decided on using very high oxidation state complexes, the problem became one of identifying the LMCT absorption bands in the electronic spectra of the complexes. Several generalities concerning the spectral features of charge-transfer absorption bands are accepted (i.e., LMCT bands are intense,[4] they shift as solvent polarity changes,[5] etc.) but these generalities are not really very useful in making detailed band assignments; we needed a reliable and routine method of identifying the LMCT absorption bands. A good calculational method seemed appropriate and we decided on using the self-consistent-field–Xα–scattered-wave (SCF–Xα–SW) molecular orbital method[6] because it has had considerable success in the elucidation of the electronic structures of low oxidation state organometallic complexes.[7]

Table I. Titanium–Halide Bond Lengths (Å) Using the Scaled Sum Method

Ti–F	Ti–Br	Ti–I	source of radii
2.01	2.51	2.70	covalent[21]
1.87	2.51	2.75	atomic[22]
1.89		2.73	Cp_2ZrX_2[23]
2.02	2.50		TiX_4[24]
1.90	2.54	2.75	GeX_4[25]
1.92	2.52	2.73	av

Table II. Structural Data for Cp_2TiL_2 and Analogous Complexes

molecule	L–M–L angle,[a] deg	Cp–M length, Å[b]	Cp–M–Cp angle, deg
Cp_2ZrF_2[23]	96.2	2.20	131.1
Cp_2ZrCl_2[23]	97.1	2.20	126.0–128.3
Cp_2ZrI_2[23]	96.2	2.19	126.0
Cp_2TiCl_2[19]	94.6	2.06	131.0
Cp_2TiS_5[26]	94.6	2.07	133.7
$Cp_2Ti(SO_3CF_3)_2$[27]	91.2	2.04	131.0
$Cp_2Ti(OCOC_6H_4NO_2\text{-}p)_2$[27]	92	2.05	132
$(\eta^5\text{-idenyl})_2Ti(CH_3)_2$[28]	92.8	2.09	119.8

[a] Refers to non-cyclopentadienyl ligands. [b] Refers to distance from metal to centroid of cyclopentadienyl ring.

In order to test the feasibility of using the SCF–Xα–SW method, we began by investigating a series of relatively well-studied complexes: the titanocene dihalide and the titanocene dimethyl complexes. Enough is known[8-11] about the Cp_2TiL_2 complexes

---

(1) The logic here is that the metal is formally reduced in the LMCT excited state: $(M^-\text{–}L^+)^*$. Certain reactions of the excited state might "keep" the electron on the metal in the product.

(2) Geoffroy, G. L.; Wrighton, M. S. "Organometallic Photochemistry"; Academic Press: New York, 1979.

(3) Beach, N. A.; Gray, H. B. *J. Am. Chem. Soc.* **1968**, *90*, 5713–5721.

(4) (a) Gray, H. B. *J. Chem. Educ.* **1964**, *31*, 1–12. (b) Ballhausen, C. J.; Gray, H. B. "Molecular Orbital Theory"; W. A. Benjamin: New York, 1965. See also ref 2 and 3.

(5) (a) Saito, H.; Fujita, J.; Saito, K. *Bull. Chem. Soc. Jpn.* **1968**, *41*, 359–364. (b) Saito, H.; Fujita, J.; Saito, K. *Ibid.* **1968**, *41*, 863–874.

(6) (a) Slater, J. C. "The Calculation of Molecular Orbitals"; Wiley: New York, 1979 and references therein. (b) Johnson, K. H. *Adv. Quantum Chem.* **1973**, *7*, 143–185 and references therein. (c) Rosch, N.; Klemperer, W. G.; Johnson, K. H. *Chem. Phys. Lett.* **1973**, *23*, 149–154. (d) Johnson, K. H.; Smith, F. C. *Phys. Rev. B* **1972**, *5*, 831–843.

(7) (a) Weber, J.; Geoffroy, M.; Goursot, A.; Penigault, E. *J. Am. Chem. Soc.* **1978**, *100*, 3995–4003. (b) Goursot, A.; Penigault, E.; Weber, J. *Nouv. J. Chim.* **1979**, *3*, 675–681. (c) Weber, J. *J. Mol. Struct.* **1980**, *60*, 397–400. (d) Balazs, A. C.; Johnson, K. H.; Whitesides, G. M. *Inorg. Chem.* **1982**, *21*, 2162–2174. (e) Ginsberg, A. P.; Osborne, J. H.; Sprinkle, C. R. *Ibid.* **1983**, *22*, 254–266. (f) Johnson, K. H. *Int. J. Quantum Chem.* **1973**, *7*, 347–351.

(8) (a) Harrigan, R. W.; Hammond, G. S.; Gray, H. B. *J. Organomet. Chem.* **1974**, *81*, 79–85. (b) Vitz, E.; Brubaker, C. H., Jr. *Ibid.* **1974**, *84*, C16–C18. (c) Vitz, E.; Brubaker, C. H., Jr. *Ibid.* **1976**, *104*, C33–C35. (d) Vitz, E.; Wagner, P. J.; Brubaker, C. H., Jr. *Ibid.* **1976**, *107*, 301–306. (e) Lee, J. G.; Brubaker, C. H., Jr. *Inorg. Chim. Acta* **1977**, *25*, 181–184. (f) Tsai, Z.; Brubaker, C. H., Jr. *J. Organomet. Chem.* **1979**, *166*, 199–210.

(9) (a) Alt, H.; Rausch, M. D. *J. Am. Chem. Soc.* **1974**, *96*, 5936–5937. (b) Rausch, M. D.; Boon, W. H.; Alt, H. G. *J. Organomet. Chem.* **1977**, *141*, 299–312. (c) Samuel, E.; Maillard, P.; Giannotti, C. *Ibid.* **1977**, *142*, 289–298. (d) Peng, M.; Brubaker, C. H., Jr. *Inorg. Chim. Acta* **1978**, *26*, 231–235. (e) Bamford, C. H.; Puddephatt, R. J.; Slater, D. M. *J. Organomet. Chem.* **1978**, *159*, C31–C33. (f) Pankowski, M.; Samuel, E. *Ibid.* **1981**, *221*, C21–C24.

(10) (a) Dias, A. R. *Rev. Port. Quim.* **1971**, *13*, 222–235. (b) Chien, J. C. W. *J. Phys. Chem.* **1963**, *67*, 2477–2481.

0002-7863/84/1506-0639$01.50/0

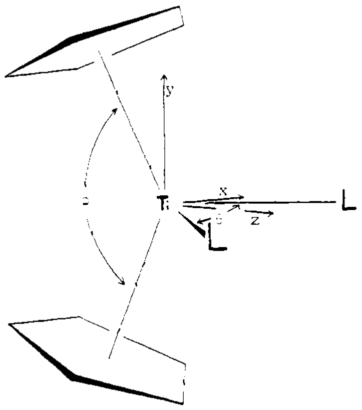

Figure 1. Coordinate system used in the SCF–Xα–SW calculations on the Cp_2TiL_2 complexes.

($Cp = \eta^5\text{-}C_5H_5$; L = F, Cl, Br, I, CH_3) that a detailed comparison of the SCF–Xα–SW results with experimental results is possible. The Cp_2TiL_2 complexes have another advantage for a first study; they are d^0 complexes. Thus, there will be no interfering d–d or MLCT transitions. This paper reports the results of our SCF-Xα–SW investigation of the Cp_2TiL_2 complexes.

Experimental Section

Calculations were carried out by the SCF–Xα–SW method.[6] Current versions of the programs were used[12] and they were run on the chemistry department's DEC VAX 11/780 computer. Norman's procedure for interpolation of overlapping sphere sizes was used to optimize the virial coefficient at one.[13,14] Relaxed optical transitions and ionization energies were calculated by using the transition-state procedure.[15] Schwarz's α_{HF} values[16] were used for the atomic exchange parameters, except for hydrogen, in which case Slater's value[17] of 0.77725 was used. The α values for the intersphere and outersphere regions were a weighted average of the atomic α values, where the weights are the number of valence electrons on the different neutral free atoms.

A minimal basis set in partial wave expansions was used for all of the calculations.[18] The use of a minimal basis set is justified on the basis of a less than 2% change in the calculated eigenvalues in going from an extended to a minimal basis set for titanocene dichloride.[18] Using the value of $l = 2$ for the outersphere region was sufficient to generate basis function components in all representations.

The coordinates of the Cp_2TiF_2, Cp_2TiBr_2, and Cp_2TiI_2 complexes had to be estimated because X-ray crystallographic data were available only for Cp_2TiCl_2.[19] Figure 1 shows the coordinate system used for the Cp_2TiL_2 complexes. All of the molecular coordinates were adjusted to idealized C_{2v} symmetry. The Ti–X (X = F, Br, I) bond lengths were estimated by using Yeranos' scaled sum formula.[20] Five sources of atomic radii were used in the calculations; the final Ti–X bond lengths used were the average of the five calculations (Table I).[21-25] The remaining structural parameters for the Cp_2TiX_2 complexes were estimated by comparing the angle and bond lengths of the Cp_2ZrX_2 complexes; the structures of the Cp_2ZrF_2, Cp_2ZrCl_2, and Cp_2ZrI_2 complexes have been determined[23] (Table II). Comparison of the structural data for this series of complexes shows that the L–Zr–L angles and the Cp–Zr bond lengths change less than 1% while the Cp–Zr–Cp angles change by less than 5%. On the basis of this observation it was assumed for the Cp_2TiX_2 complexes that the L–Ti–L angles, the Cp–Ti–Cp angles, and the Cp–Ti bond lengths would not vary significantly. For this reason, the structural parameters for the Cp_2TiCl_2 complex were used for all of the complexes.

Table III. Experimental[10] and Calculated[a] Electronic Transition Energies[b] and Assignments for Titanocene Dihalides

molecule		$10b_2 \rightarrow 14a_1$[c]	$9b_1 \rightarrow 14a_1$[c]	$6a_2 \rightarrow 14a_1$[d]	$13a_1 \rightarrow 14a_1$[c]
Cp_2TiF_2	exptl	3.2	3.8		
	calcd	2.0	2.4	2.4	2.8
Cp_2TiCl_2	exptl	2.4	3.2		3.9
	calcd	1.7	2.1	2.2	2.6
Cp_2TiBr_2	exptl	2.3	2.9		3.8
	calcd	1.5	1.9	2.0	2.4
Cp_2TiI_2	exptl	*e*	*e*		*e*
	calcd	1.4	1.7	1.9	2.3

[a] Spin-restricted transition-state SCF–Xα-SW calculation.
[b] Energy in eV. [c] Symmetry allowed. [d] Symmetry forbidden.
[e] See text for discussion of Cp_2TiI_2 assignments.

Table IV. Experimental[11b] and Calculated[a] Ionization Energies[b] and Assignments for Titanocene Dichloride

exptl	calcd	orbital; character[c]
8.5	7.6	$10b_2$; Cp, Ti
8.9	7.9	$9b_1$; Cp, Ti
9.1	8.1	$6a_2$; Cp, Ti
9.9	8.5	$13a_1$; Cp, Ti
10.2	10.0	$8b_1$; Cl
10.7	10.4	$9b_2$; Cl
11.1	10.6	$5a_2$; Cl

[a] Spin-restricted transition-state SCF–Xα-SW calculation.
[b] Energy in eV. [c] See text for discussion of orbital character.

The coordinates of the $Cp_2Ti(CH_3)_2$ complex were obtained from the molecular structures of several analogous complexes[26-28] (Table II). Notice in Table II that the structural features of the Cp_2Ti fragments are all very similar. Also note that the structure of the $(\eta^5\text{-indenyl})_2Ti(CH_3)_2$ complex is known.[28] In this complex the Ti–CH_3 bond length is 2.21 Å and the CH_3–Ti–CH_3 angle is 92.8°. This latter value is very similar to the Cl–Ti–Cl angle in Cp_2TiCl_2 (94.6°). Therefore, all angles and bond lengths for the $Cp_2Ti(CH_3)_2$ complex were taken from the Cp_2TiCl_2 complex except the Ti–CH_3 bond length, which was assumed to be identical with the Ti–CH_3 bond length in $(\eta^5\text{-indenyl})_2Ti(CH_3)_2$. The exact coordinates for all of the complexes (including outersphere coordinates) are available as supplementary material.[29]

---

(11) (a) Lauher, J.; Hoffmann, R. *J. Am. Chem. Soc.* **1976**, *98*, 1729-1742. (b) Cauletti, C.; Clark, J. P.; Green, J. C.; Jackson, S. E.; Fragala, I. L.; Ciliberto, E.; Coleman, A. W. *J. Electron Spectrosc.* **1980**, *18*, 63-73. (c) Ballhausen, C. J.; Dahl, J. P. *Acta Chem. Scand.* **1961**, *15*, 1333-1336. (d) Green, J. C.; Green, M. L. H.; Prout, C. K. *Chem. Commun.* **1972**, 421-422. (e) Green, M. L. H. *Pure Appl. Chem.* **1972**, *30*, 373-388. (f) Peterson, J. L.; Dahl, L. F. *J. Am. Chem. Soc.* **1974**, *96*, 2248-2250. (g) Peterson, J. L.; Dahl, L. F. *Ibid.* **1975**, *97*, 6416-6422. (h) Peterson, J. L.; Dahl, L. F. *Ibid.* **1975**, *97*, 6422-6432. (i) Green, J. C.; Jackson, S. E.; Higginson *J. Chem. Soc., Dalton Trans.* **1975**, 403-409. (j) Alcock, N. W. *J. Chem. Soc. A* **1967**, 2001-2009.

(12) The programs were received from K. H. Johnson in 1981 and converted for use on a DEC VAX 11/780 by W. H. Klemperer and M. R. Bruce.

(13) (a) Norman, J. G., Jr. *J. Chem. Phys.* **1974**, *61*, 4630-4635. (b) Norman, J. G., Jr. *Mol. Phys.* **1976**, *31*, 1191-1198.

(14) In practice, the program calculates the ratio of atomic radii and varies the percent of the calculated atomic radii while holding the ratio fixed to be used in the molecular potential. Limited computer time necessitates close but non-one virial coefficients. For Cp_2TiF_2, Cp_2TiCl_2, Cp_2TiBr_2, Cp_2TiI_2, and $Cp_2Ti(CH_3)_2$ the converged virial coefficients were 1.000172, 1000124, 1000089, 1.000063, and 1.000404, respectively.

(15) See ref 6a, 49-53.

(16) (a) Schwarz, K. *Phys. Rev. B* **1972**, 2466-2468. (b) Schwarz, K. *Theor. Chim. Acta* **1974**, *34*, 225-231. (Iodine's Xα value (0.70078) was found by interpolation.)

(17) Slater, J. C. *Int. J. Quantum Chem.* **1973**, *7*, 533-544.

(18) Minimal basis set for Cp_2TiL_2: Ti, $l = 2$; C, $l = 1$; H, $l = 0$; F, $l = 1$; Cl, $l = 1$; Br, $l = 2$; I, $l = 2$; Extended basis set for Cp_2TiCl_2: Ti, $l = 3$; C, $l = 2$; H, $l = 1$; Cl, $l = 2$.

(19) (a) Clearfield, A.; Warner, D. K.; Saldarriaga-Molina, C. H. Ropal, R.; Bernal, I. *Can. J. Chem.* **1975**, *53*, 1622-1629. (b) Peterson, J. L.; Lichtenberger, D. L.; Fenske, R. F.; Dahl, L. F. *J. Am. Chem. Soc.* **1975**, *97*, 6433-6441 and references therein.

(20) Yeranos, W. A.; Foss, F. D. *Mol. Phys.* **1965**, *9*, 87-96.

(21) Pauling, L. "Nature of the Chemical Bond"; 3rd ed.; Cornell University Press: Ithaca, NY, 1960.

(22) Slater, J. C. "Quantum Theory of Molecules and Solids"; McGraw-Hill: 1965; Vol. 2, p 55.

(23) Prout, K.; Cameron, T. S.; Forder, R. A. *Acta Crystallogr., Sect. B* **1974**, *B30*, 2290-2304 and references therein.

(24) Kimura, M.; Kimura, K.; Aoki, M.; Shibata, S. *Bull. Chem. Soc. Jpn.* **1956**, *29*, 95-100.

(25) Wells, A. F. "Structural Inorganic Chemistry"; Clarendon Press: Oxford, 1975; p 728.

(26) Epstein, E. F.; Bernal, I.; Kopf, H. *J. Organomet. Chem.* **1971**, *26*, 229-245.

(27) Klein, H.; Thewalt, U. *J. Organomet. Chem.* **1981**, *206*, 69-75.

(28) Atwood, J. L.; Hunter, W. E.; Hrncir, D. C.; Samuel, E.; Alt, H.; Rausch, M. D. *Inorg. Chem.* **1975**, *14*, 1757-1762.

(29) See end of text for ordering information.

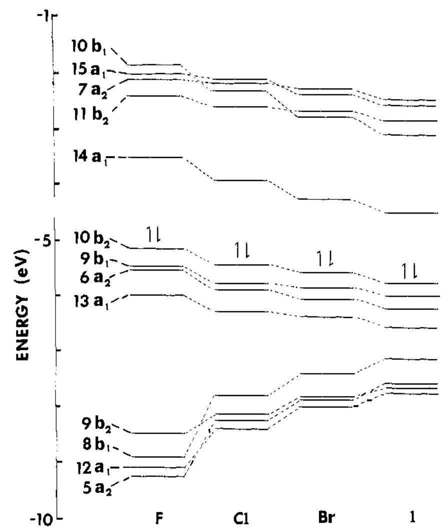

Figure 2. Eigenvalues for the Cp_2TiX_2 (X = F, Cl, Br, I) complexes. The pair of electrons in the $10b_2$ orbital indicates the highest occupied molecular orbital.

Results

Titanocene Dihalides. Figure 2 shows the ground-state eigenvalues and symmetries of selected titanocene dihalide orbitals. The orbitals of interest can be grouped into three sets: a set of lowest unoccupied molecular orbitals (LUMO's ≡ $14a_1$, $11b_2$, $7a_2$, $15a_1$, $10b_1$) that is stabilized in going from Cp_2TiF_2 to Cp_2TiI_2, a set of highest occupied molecular orbitals (HOMO's ≡ $13a_1$, $6a_2$, $9b_1$, $10b_2$) that is stabilized in going from Cp_2TiF_2 to Cp_2TiI_2, and a set of lower lying occupied molecular orbitals (LOMO's ≡ $5a_2$, $12a_1$, $8b_1$, $9b_2$) that is destabilized faster than the HOMO and LUMO orbital sets are stabilized.

Contour plots of the molecular wave functions for the LUMO set clearly indicate they are primarily titanium d orbitals. In C_{2v} symmetry, the d orbitals transform as follows: $d_{x^2-y^2}$, a_1; d_{z^2}, a_1; d_{xy}, a_2; d_{xz}, b_1; d_{yz}, b_2. The $11b_2$, $10b_1$, and $7a_2$ orbitals are the titanocene d_{yz}, d_{xz}, and d_{xy} orbitals, respectively. The $14a_1$ and $15a_1$ molecular orbitals are mixtures of the $d_{x^2-y^2}$ and d_{z^2} orbitals. At one time there was considerable disagreement as to the bonding and the relative energies of the d orbitals in bent metallocenes.[11c] However, as a result of experimental and theoretical studies, there is now general agreement on the relative energies of the d orbitals in those complexes.[11] The relative d-orbital energies that we obtain are similar to those agreed upon by others.

As photochemists, of course, we are not just interested in the LUMO orbitals but also in the HOMO orbitals. Contour plots for the HOMO set of orbitals show that these orbitals are predominantly cyclopentadienyl and titanium in character with a small amount of halide orbital mixed in. A representative set of contour plots of interest to the low-energy photochemistry is shown in Figure 3 for the Cp_2TiCl_2 complex. Two types of plots are shown.[30] First, the *xz*, *yz*, and *xy* planes are illustrated. Next, a plane that contains the titanium and one chlorine atom and that is perpendicular to the *xz* plane is shown. (This plane is labeled Ti–Cl in Figure 3.) Contour plots of the molecular wave functions for the LOMO set of orbitals show that these molecular orbitals are all predominantly halide in character. Other orbital plots are found in the supplementary material.[29]

Table III shows the calculated and experimental electronic transition energies for the Cp_2TiX_2 complexes. The experimental energies found in Table III for Cp_2TiX_2 are those reported by Dias and Chien.[10] Table IV shows the calculated and experimental ionization energies for Cp_2TiCl_2. The experimental ionization energies are those reported by Green and co-workers.[11b]

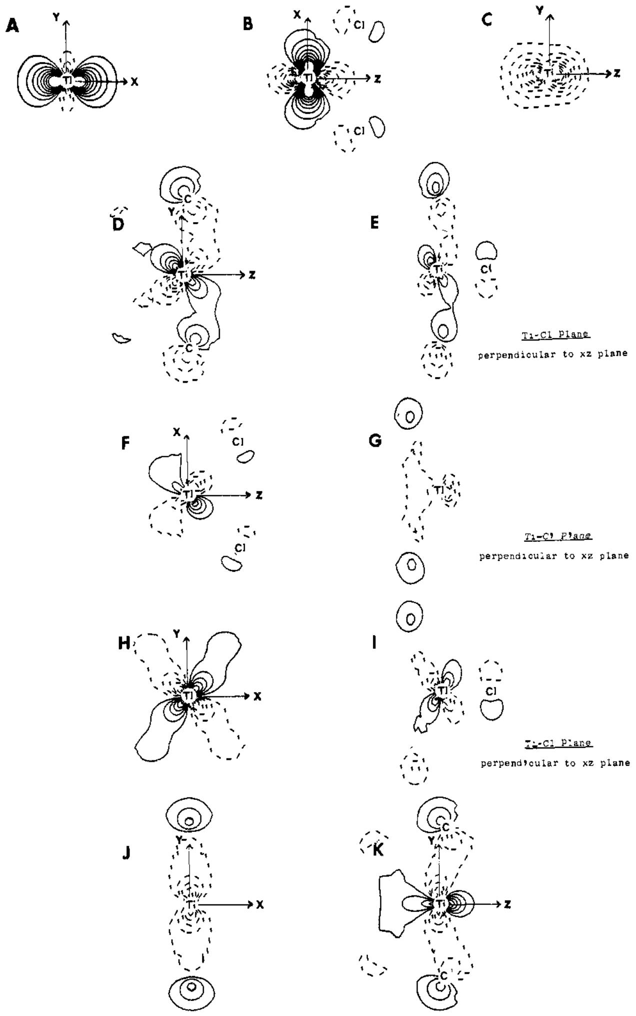

Figure 3. Wave function countour plots for Cp_2TiCl_2: (A) $14a_1$, *xy* plane; (B) $14a_1$, *xz* plane; (C) $14a_1$, *yz* plane; (D) $10b_2$, *yz* plane; (E) $10b_2$, TiCl plane; (F) $9b_1$, *xz* plane; (G) $9b_1$, TiCl plane; (H) $6a_2$, *xy* plane; (I) $6a_2$, TiCl plane; (J) $13a_1$, *xy* plane; (K) $13a_1$, *yz* plane. Solid and broken lines denote contours of opposite sign at values of ±0.05, ±0.10, ±0.15, ±0.20, ±0.25, ±0.30, ±0.35, ±0.40 $e^{1/2}$ $bohr^{-3/2}$, respectively.

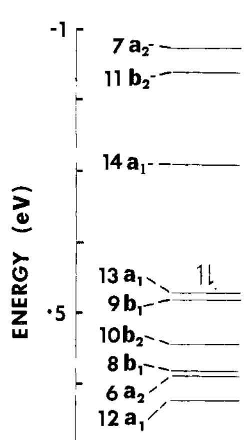

Figure 4. Eigenvalues for Cp_2TiMe_2 [Me = CH_3]. The pair of electrons in the $13a_1$ orbital indicates the highest occupied molecular orbital.

Dimethyltitanocene. Figure 4 shows the ground-state eigenvalues and orbital symmetries for the titanocene dimethyl complex. A representative set of contour plots of interest to the low-energy photochemistry is shown in Figure 5.[30] The key results are the following. The lowest unoccupied set of orbitals ($7a_2$, $11b_2$, $14a_1$) is primarily the titanium d_{xy} orbital, the d_{yz} orbital, and an orbital

---

(30) Coordinate axes have been drawn only for contour plots in the *xz*, *yz*, and *xy* planes. Those atoms that are in the plane are labeled as follows: Ti = titanium, Cl = chlorine, C = carbon in cyclopentadienyl ring, and Me = carbon in methyl group.

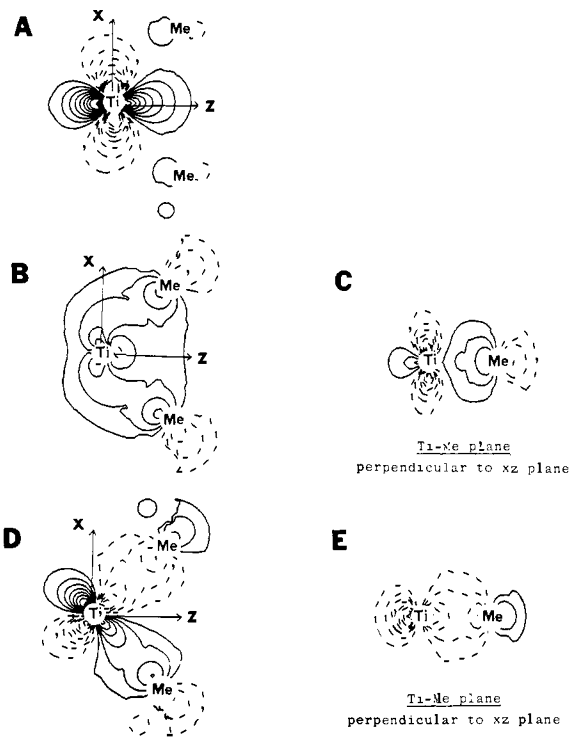

Figure 5. Wave function contour plots for $Cp_2Ti(CH_3)_2$: (A) $14a_1$, xz plane; (B) $13a_1$, xz plane; (C) $13a_1$, TiMe plane; (D) $9b_1$, xz plane; (E) $9b_1$, TiMe plane. See Figure 3 for contour values.

that is a mixture of the d_{z^2} and $d_{x^2-y^2}$ orbital, respectively. The highest occupied set of orbitals ($13a_1$, $9b_1$) is primarily methyl in character with significant d-orbital character. The Ti-Me plane is analogous to the Ti–Cl plane. The orbitals immediately below the $13a_1$ and $9b_1$ orbitals in energy ($10b_2$, $8b_1$, $6a_2$, $12a_1$) are all primarily cyclopentadienyl in character. Additional results pertaining to all of the calculations are available as supplementary material.[29]

Discussion

The SCF-Xα-SW method was chosen as our computational method because it is a nonparameterized method. Despite some limitations[31] the method seemed to be the best available for gaining insights into the photochemical reactions of LMCT excited states. Other methods (notably the CNDO method[32]) can give results qualitatively similar to our SCF-Xα-SW results on the Cp_2TiL_2 complexes, but these other methods are extensively parameterized. They are thus unsuitable for our studies because in most cases the data are not available to parameterize our calculations. Additionally, previous molecular orbital calculations on Cp_2TiCl_2 have given contradictory results.[19b,32]

The key results from our calculations on the Cp_2TiX_2 (X = F, Cl, Br, I) complexes are the following. (1) The two lowest energy transitions in these complexes are predicted to be predominantly Cp → Ti in character. (2) The calculated ionization energies for the Cp_2TiCl_2 complex are in good agreement with the experimentally observed values.[11b] (3) There are certain trends in the energies of the orbitals as the halide is changed from fluoride to chloride to bromide to iodide. Specifically, the energy of the LUMO orbital (a d orbital on the Ti) decreases in energy along the series. The higher energy (also unoccupied) d orbitals also decrease in energy. In addition, the four highest energy occupied orbitals (primarily Cp in character) also become more stable (decrease in energy) but the decrease is not so pronounced as it is in the case of the HOMO orbital. The overall effect is thus to decrease the energy gap between the HOMO set and the LUMO along the series. Lastly, the energies of the LOMO set of orbitals ($5a_2$–$9b_2$) increase dramatically in going from fluoride to iodide. Thus, whereas the energy gap between the fluoride and Cp orbitals in Cp_2TiF_2 is about 2.4 eV, the energy gap between the corresponding iodide and Cp orbitals in the Cp_2TiI_2 complex is about 0.5 eV. The implications of these results for the photochemistry of these complexes will now be discussed.

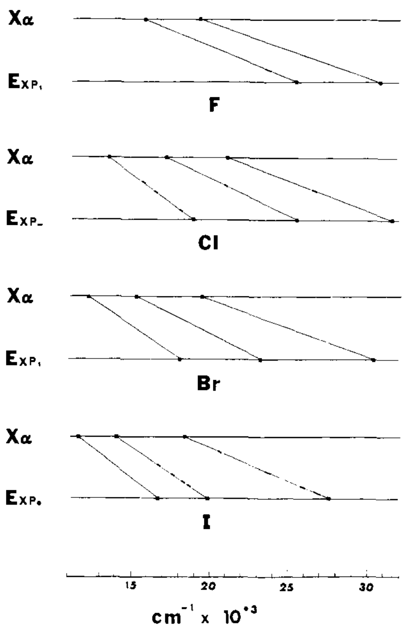

Figure 6. Xα transition state vs. experimental transition energies for Cp_2TiX_2 [X = F, Cl, Br, I]. Only allowed transitions are shown. For experimental results see ref 10.

For all of the halide complexes, the lowest energy excited states are predicted to be those arising from population of the $14a_1$ orbital and depopulation of the $10b_2$, $9b_1$, and $13a_1$ orbitals, giving rise to $^1A_1 \rightarrow {}^1B_2$, $^1A_1 \rightarrow {}^1B_1$, and $^1A_1 \rightarrow {}^1A_1$ transitions, respectively. (The $6a_2 \rightarrow 14a_1$ ($^1A_1 \rightarrow {}^1A_2$) transition is not allowed). The four highest energy occupied molecular orbitals are predominantly Cp and Ti in character; the $10b_2$, $13a_1$, and $6a_2$ orbitals are Cp–Ti bonding and the $9b_1$ orbital is Cp–Ti nonbonding (Figure 3, D–K). The $14a_1$ orbital is primarily a d orbital ($x^2 - y^2$, z^2 mixture), and it is Ti–X antibonding and essentially Ti–Cp nonbonding (Figure 3, A–C). Two conclusions can be drawn. First, the lowest energy electronic transitions in the Cp_2TiX_2 complexes can be characterized as Cp → Ti charge-transfer transitions. Second, irradiation of these complexes in the lowest energy electronic absorption bands will weaken the Ti–Cp bonds because a Ti–Cp bonding orbital is being depopulated. These two conclusions are consistent with the known photochemistry of the Cp_2TiCl_2 and Cp_2TiBr_2 complexes.[8] Extensive studies by Brubaker and co-workers and other studies show that irradiation of the chloride and bromide complexes in the lowest energy absorption bands leads to Ti–Cp bond cleavage.[8] Our calculations provide an excellent rationale for this behavior.

The second noteworthy result mentioned above concerns the calculated ionization potentials for the Cp_2TiCl_2 complex. As shown in Table IV the agreement with the experimental results is very good. Green and co-workers[11b] have shown that the orbitals for the first four ionizations are Cp in character, while the next three have predominantly halogen character. This is in agreement with our results. More important to the photochemist than the ability to calculate ionization energies is the ability to accurately calculate or predict the electronic transition energies so as to interpret the electronic spectrum. The electronic spectral features of the Cp_2TiX_2 complexes are summarized in Table III. Figure 6 compares the overall pattern of experimental optical transition energies to the calculated transition energies. It is apparent that

---

(31) (a) Salahub, D. R.; Foti, A. E.; Smith, V. H., Jr. *J. Am. Chem. Soc.* **1978**, *100*, 7847–4859. (b) Slater, J. C. *Adv. Quantum Chem.* **1972**, *6*, 1–53. (c) See ref 13b. (d) Case, D. A. *Annu. Rev. Phys. Chem.* **1982**, *33*, 151–171. (e) Danese, J. B.; Connolly, J. W. D. *J. Chem. Phys.* **1974**, *61*, 3063–3070. (f) Kaufman, J. J. *Int. J. Quantum Chem. Symp.* **1973**, *7*, 369–370.

(32) Condorelli, G.; Fragala, I.; Centineo, A.; Tondello, E. *J. Organomet. Chem.* **1975**, *87*, 311–315.

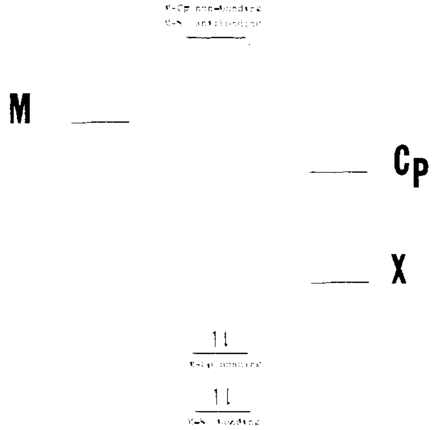

Figure 7. Simplified molecular orbital diagram for the interaction of a Cp orbital and a halide orbital with a metal orbital.

the SCF–Xα–SW calculated transition energies are red shifted with respect to the experimental values, but the pattern of the transitions (i.e., the energy spacings between the peaks) predicted by the calculation is in excellent agreement with the experimental pattern. Thus, while the SCF–Xα–SW method may fail in predicting the absolute energies of LMCT transitions, it is a useful tool in analyzing spectral trends. This use, recall, is our primary reason for using the SCF–Xα–SW method, and we fell the results on the Cp_2TiX_2 complexes justifies its continued use in our study of LMCT excited states.

The third key result mentioned above concerns several of the orbital trends as the halide is change from fluoride to chloride to bromide to iodide. In analyzing these trends it is easiest to think of the orbital interactions as shown in the simplified diagram in Figure 7. In this figure, a single Cp orbital and a single halide orbital (X) are shown interacting with a single metal d orbital. The interaction produces three molecular orbitals as shown. In keeping with the results of the Xα calculation, the highest energy molecular orbital in the simplified scheme is primarily a metal orbital, the lowest energy molecular orbital is mostly halide in character, and the middle energy orbital is primarily a Cp orbital. By referring to this simple scheme, it is an easy matter to explain the trends in the series of calculations on the Cp_2TiX_2 complexes. The first trend to explain is the decreasing energy of the d orbitals along the series. Note that the d orbitals generally drop in energy in going from the fluoride to the iodide complex. The d orbitals are stabilized because there is less Ti–X interaction along the series. This point is illustrated in Figure 8A, B, which shows the change in molecular wave functions for Cp_2TiCl_2 vs. Cp_2TiI_2. (The contours in Figure 8 are of much lower densities than those in previous figures). Clearly, there is more Ti–X interaction in the chloride complex than in the iodide complex. The decreasing Ti–X interaction stabilizes the metal d orbitals because the d orbital is Ti–X antibonding.

The Ti–X bonding orbital is the lowest energy orbital in our scheme (primarily halide in character); as the Ti–X interaction decreases, it will increase in energy. Note that the halide orbitals do rise in energy along the series, and the decreasing metal–halide interaction is probably partially responsible for the increase (Figure 8C,D). However, the major factor is most likely the changing halogen atom itself; the energies of the valence orbitals on the halogen atom will increase in going down the halogen family from fluorine to iodine, and this increase in the valence orbital energies is reflected in the energies of the molecular orbitals that are primarily halide in character.

Finally, note that the Cp orbitals decrease in energy in going from fluoride to iodide. The decrease is slight compared to the LUMO orbital, and hence, there is a red shift of the lowest energy Cp → Ti charge-transfer absorption bands. The Cp orbitals decrease in energy because they are metal–halide antibonding and metal–cyclopentadienyl bonding. Thus, as the metal–halide interaction decreases, these orbitals will decrease in energy because they are less antibonding; the Cp–metal (bonding) interaction increases along the series, further depressing the energy of these orbitals (Figure 8E,F).

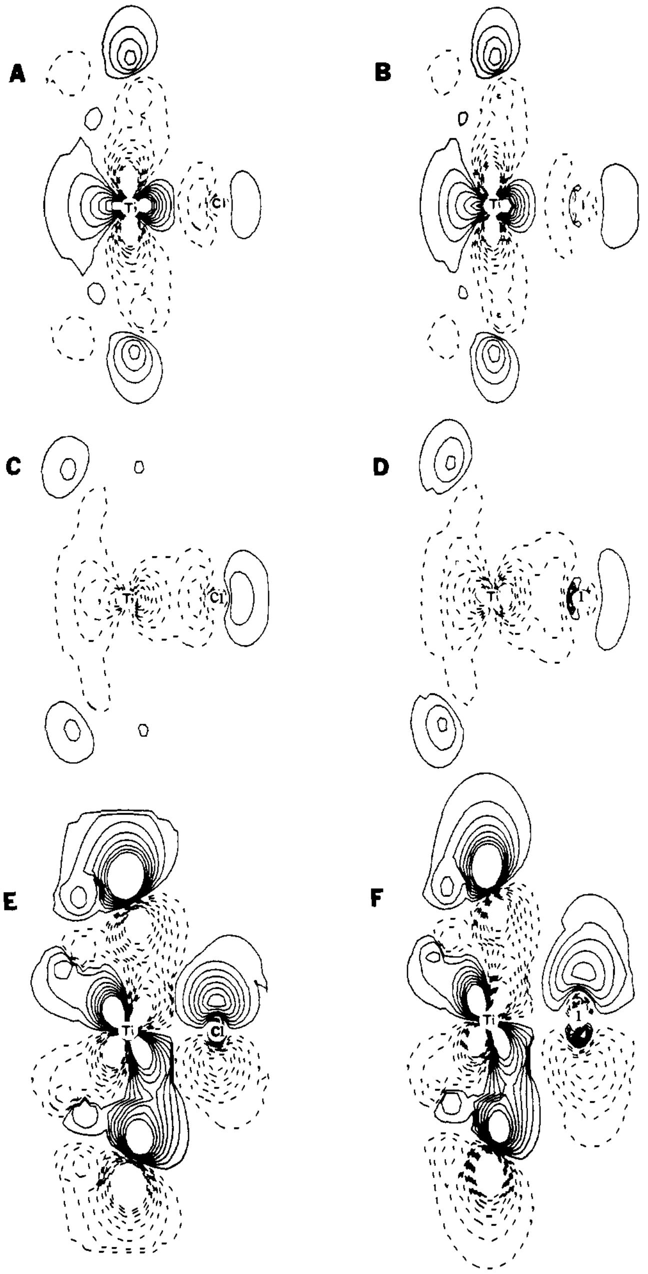

Figure 8. Comparisons of wave function contour plots of Cp_2TiX_2 [X = Cl, I]: (A) $14a_1$, Cp_2TiCl_2, TiCl plane; (B) $14a_1$, Cp_2TiI_2, TiI plane; (C) $8b_1$, Cp_2TiCl_2, TiCl plane; (D) $8b_1$, Cp_2TiI_2, TiI plane; (E) $10b_2$, Cp_2TiCl_2, TiCl plane; (F) $10b_2$, Cp_2TiI_2, TiI plane; Solid and broken lines denote contours of opposite sign at values of ±0.01, ±0.02, ±0.03, ±0.04, ±0.05, ±0.06, ±0.07, ±0.08 $\text{electron}^{1/2}\ \text{bohr}^{-3/2}$, respectively.

What are the implications of the various trends just discussed? Spectroscopically speaking, the most noticeable trend is the decreasing energy gap between the HOMO and LUMO orbitals. This is the cause of the red shift in the electronic spectra of the Cp_2TiX_2 complexes along the series fluoride to iodide. Without other evidence (i.e., known photochemistry or calculational results), one might conclude that the two lowest energy absorption bands were halide-to-metal charge-transfer bands because a red shift would be expected as the halide became more polarizable (as is the case in going from fluoride to iodide). On the basis of the known photochemistry of these complexes and on the basis of our calculational results, we are confident in assigning the two lowest energy electronic transitions in these complexes to Cp → Ti charge transfer, at least in the case of the fluoride and chloride complexes

(Table III).

There is some ambiguity in the assignment of the lowest energy transitions in the bromide and iodide complexes. Because the Cp orbitals drop in energy and the halide orbitals rise in energy along the series, it is obvious that at some point the two series of orbitals will meet and intertwine with each other; perhaps the halide orbitals will even eventually rise above the Cp orbitals. In our calculation the trend toward the orbitals meeting is clear but the two types of orbitals have not met and are still separate even in the iodide complex. The UV photoelectron spectral results of Green and co-workers,[11b] however, suggest that in the bromide complex the two types of orbitals are very close in energy and in the iodide complex the iodide orbitals are higher in energy than the Cp orbitals. When the Cp_2TiBr_2 complex is irradiated in its lowest energy electronic absorption band, the Cp–Ti bonds are cleaved.[8a] On the basis of this result we suggest that a Cp → Ti charge-transfer transition is still lowest in energy in this complex. Adhering to our belief of not using the SCF–Xα–SW method for purposes for which it was not intended, we concede that the results of our calculation probably cannot determine which set of orbitals is the higher one in the iodide complex. The point, however, is that the calculation predicts that the Cp and halide orbitals will come closer together along the series. This trend is enough to alert us that the lowest energy excited states of the iodide complex (and possibly the bromide complex) may be different from the earlier members of the series and that the photochemistry of the iodide complex may be different as well. This latter prediction has been borne out; an investigation in our laboratory of the photochemistry of the Cp_2TiI_2 complex shows that the Cp–Ti bonds do not break when this complex is irradiated.[33] Instead, the Ti–I bonds are cleaved.[33] The different photochemistry of the iodide complex is probably a consequence of having a different lowest energy, photochemically active excited state. On the basis of our experimental results and the trend found in the calculations, we assign the lowest energy transition in the Cp_2TiI_2 complex to an iodide-to-Ti charge transfer ($8b_1 \rightarrow 14a_1$; $^1A_1 \rightarrow {}^1B_2$). In the absence of detailed spectroscopic data, it makes no sense to assign the other bands in the iodide complex.

The calculational results on the $Cp_2Ti(CH_3)_2$ complex also support our claim that the SCF–Xα–SW method will be useful in identifying LMCT electronic absorption bands. The two lowest energy excited states for this complex are predicted to be $13a_1 \rightarrow 14a_1$ and $9b_1 \rightarrow 14a_1$ ($^1A_1 \rightarrow {}^1A_1$ and $^1A_1 \rightarrow {}^1B_1$, respectively). The $13a_1$ and $9b_1$ orbitals are Ti–CH_3 bonding orbitals and the $14a_1$ orbital is a titanium d orbital (a d_{z^2}, $d_{x^2-y^2}$ mixture) (Figure 5). The important point here is that the lowest energy excited states are not Cp → Ti charge transfer, as in the fluoride, chloride, and bromide complexes, but are transitions involving the Ti–CH_3 σ bond. On the basis of this result we might expect the photochemical behavior of the $Cp_2Ti(CH_3)_2$ complex to be very different from that of the halide complexes. In fact, the photochemical reactivities of the two types of complexes are very different. Whereas the Cp–Ti bonds are photochemically cleaved in the Cp_2TiX_2 complexes (X = F, Cl, Br), the Ti–CH_3 bonds are cleaved in the $Cp_2Ti(CH_3)_2$ complex.[9] (Cleavage of the Ti–CH_3 bond appears not to involve formation of free methyl radicals.[9] The point is, however, that the Ti–CH_3 bond is ultimately broken.)

Acknowledgment. We thank Professor Walter Klemperer for teaching us about the Xα method. This work was supported by a University Exploratory Research Grant from the Procter and Gamble Co. and by a Cottrell Grant from the Research Corp.

Registry No. Cp_2TiF_2, 309-89-7; Cp_2TiCl_2, 1271-19-8; Cp_2TiBr_2, 1293-73-8; Cp_2TiI_2, 12152-92-0; $Cp_2Ti(CH_3)_2$, 1271-66-5.

Supplementary Material Available: The exact coordinates for all of the complexes, including outersphere coordinates, and other molecular orbital plots (55 pages). Ordering information is given on any current masthead page.

---

[33] Bruce, M. R. M.; Tyler, D. R., unpublished results.

Photolysis of $Re_2(CO)_{10}$ in the Presence of Simple Olefins. Thermal Reactivity of (μ-Hydrido)(μ-alkenyl)dirhenium Octacarbonyl Compounds[1]

Philip O. Nubel and Theodore L. Brown*

Contribution from the School of Chemical Sciences, University of Illinois, Urbana, Illinois 61801.
Received May 12, 1983

Abstract: Photolysis of $Re_2(CO)_{10}$ at 25 °C in the presence of ethylene, terminal olefins, or 2-butene results in formation of (μ-hydrido)(μ-alkenyl)dirhenium octacarbonyl complexes in high yield. The bridging alkenyl ligand forms a σ bond to one Re and a π bond to the other. The reaction is proposed to proceed through a light-induced radical pathway, producing a 1,2-$Re_2(CO)_8(\eta^2\text{-olefin})_2$ intermediate that undergoes thermal reaction to give the observed product. The μ-alkenyl ligand undergoes a rapid fluxional process at room temperature in which the σ and π bonds of the alkenyl group are interchanged between the bridged rhenium atoms. The μ-hydrido–μ-alkenyl compounds react with a variety of substrates under mild thermal conditions. Treatment with pyridine, $P(OMe)_3$, or $P(OPh)_3$ results in elimination of olefin and formation of 1,2-*eq*,*eq*-$Re_2(CO)_8L_2$. Kinetics investigations of reactions with pyridine are consistent with a mechanism that begins with intramolecular C–H reductive elimination. Treatment with bis(diphenylphosphino)methane (dppm) affords a dppm-bridged complex, $Re_2(CO)_8(dppm)$; reaction with PPh_3 or $P(n\text{-Bu})_3$ initially generates 1,2-*ax*,*eq*-$Re_2(CO)_8L_2$, which thermally isomerizes to 1,2-*ax*,*ax*-$Re_2(CO)_8L_2$. Nucleophilic attack of PMe_3 upon the ethenyl ligand of (μ-H)(μ-$CH{=}CH_2$)$Re_2(CO)_8$ results in a dipolar addition product. The μ-hydrido, μ-alkenyl compounds react with ethylene, terminal olefins, or *cis*-2-butene to afford the hydride- and alkenyl-exchanged hydrido–alkenyl species. Reaction with H_2 generates $H_2Re_2(CO)_8$.

The photochemistry of $Mn_2(CO)_{10}$ and $Re_2(CO)_{10}$ has been studied extensively within the past several years, particularly with respect to substitution by phosphorus[2] and, to a lesser extent, nitrogen[3] ligands. Substitution has also been effected by thermal